MODELLING OF TWO-PHASE EXPANSION IN A RECIPROCATING EXPANDER

Xander van Heule[1]*, Anastasios Skiadopoulos[2], Dimitrios Manolakos[2], Michel De Paepe[1], Steven Lecompte[1]

[1]Ghent University ,Department of Electromechanical, systems and Metal Engineering, Sint-Pietersnieuwstraat 41 Ghent, Belgium

[2]Agricultural University of Athens, Department of Agricultural Engineering, Iera Odos street 75 Athens, Greece

*Corresponding Author: xander.vanheule@ugent.be
tskiado@aua.gr
dman@aua.gr
michel.depaepe@ugent.be
steven.lecompte@ugent.be

ABSTRACT

Two-phase expansion devices are used in a multitude of cycles and allow for an increase of the overall system efficiency. It has been shown that the trilateral flash cycle can improve the power output from the recovery of low temperature residual heat compared to the classic subcritical Organic Rankine cycle. Theoretical studies predict an improvement of at least 15%. The expanders that are mainly investigated for the purpose of two-phase expansion are the Lysholm and the reciprocating expanders. From these two, the reciprocating expander has been researched the least as it is not as easy to model. It has been shown that to model the reciprocating expander, there is a need to describe the non-equilibrium state of the phases during the expansion process. This study aims to fill the knowledge gap that exists for two-phase reciprocating expanders, by constructing a predictive model to describe the expansion process and the non-equilibrium phenomena occurring. The constructed model makes use of the homogeneous relaxation model to describe the thermal non-equilibrium between the phases. The working fluid used in initial modelling is cyclopentane. The resulting model will be used to formulate design guidelines for the construction of a two-phase reciprocating expander. This prototype will be used to gain experimental data, with which the theoretically predicted efficiency improvement can be validated.

1 INTRODUCTION

Two-phase expansion processes have gathered increased interest over the past years. One of the main application areas for these types of expanders is in the recuperation of low grade heat such as in the automotive industry (Glavatskaya *et al., 2012*), geothermal heat to power, waste heat recuperation and many more. This heat can be recuperated by the use of Organic Rankine cycles (ORC) or variants thereof. Examples of variants that incorporate a two-phase expander are the Trilateral Cycle (TLC) and the Partial Evaporation ORC (PEORC). The difference between the basic ORC and the examples given is that the evaporator no longer fully evaporates the working fluid, instead it only preheats the liquid to saturation (TLC) or partly evaporates the working fluid (PEORC). In either case the expander will expand the working fluid through the two-phase region. Dipippo (2007) showed that the TLC has a lower upper bound for maximum thermal efficiency compared to the standard Carnot efficiency. Even though the thermal efficiency is intrinsically lower, the overall power output can be higher. This is a result of the better heat recovery potential due to the improved fit of the working fluid and heat carrier temperature profiles (Lecompte *et al., 2015*). Therefore, instead of the thermal efficiency, the exergy efficiency for power production is often used as a comparative value. This value is defined as the ratio of the net power production to the incoming exergy flow of the heat carrier. Fischer (2011) used this quantity to compare the Trilateral and Organic Rankine cycles and concluded that it is larger, in the range of 14% to 29%, for the TLC in all tested conditions. Another quantity used by Fischer (2011) to

compare the two cycles is the total exergy efficiency, defined as the ratio of total outgoing exergy flows to total ingoing exergy flows. The difference between the ORC and the TLC based on this definition is smaller when compared to the exergy efficiency of power production difference. In most tested operation conditions the total exergy efficiency was slightly (1 to 9%) larger for the TLC compared to the ORC. But for one operating point the total exergy efficiency was 1% higher for the ORC compared to the TLC. Another comment from the authors is that the volumetric flow rates were a lot larger for the TLC in comparison to the ORC for the same operating point. Li *et al.* (2017) compared both cycles as well, the authors concluded that the TLC has a larger power output, thermal efficiency and exergy efficiency for evaporation temperatures around 150°C. The authors also note that the large exergy destruction of an ORC, mainly due to the evaporator temperature profile mismatching, is a problem.

In current literature only two types of expanders are under consideration for the use in a TLC. These being the Lysholm or screw expander and the reciprocating or piston expander. In this research, it was opted to look more closely at the reciprocating expander. Firstly, because this expander type has an easier chamber geometry to study compared to screw expanders. Secondly the build in volume ratio (BIVR) of a reciprocating expander is the largest compared to other types of volumetric expanders (Dumont *et al., 2017*). This property lines up with the needs of a TLC, as the expander accommodates the evaporation, requiring higher volume ratios compared to ORC's. The drawback of this type of expander is the lack of relevant available experimental data. In comparison, Öhman and Lundqvist (2013) suggested that Lysholm turbine performance in two-phase operating conditions can be estimated without the expensive two-phase experimental tests. For reciprocating expanders the only available experiments were executed by Kanno and Shikazono (2015).

In this work the available model (Lecompte *et al.*, 2017) will be expanded. This available model applies the homogeneous equilibrium model (HEM) throughout the expansion process within a reciprocating expander. This implies that the working fluid is assumed to be in an equilibrium state at every time step. This methodology is sufficient for the initial raw sizing of an experimental setup, but is not completely accurate. For example, it is clearly visible in the experiments of Kanno and Shikazono (2015) that the liquid has a higher temperature in comparison to the vapour during expansion in a reciprocating expander. Indicating that the complete evaporation to equilibrium requires more time than the piston expansion. This is similar to the principle of flash evaporation under a sudden pressure drop. The adapted model uses the homogeneous relaxation model (HRM) instead of the HEM. This model incorporates the thermal non-equilibrium of the fluid within each time step. Other possible modelling techniques that incorporate thermal non-equilibrium will be discussed in the next section. Afterwards the implementation of the chosen model is further elaborated.

2 FLASHING MODELLING TECHNIQUES

There are a multitude of modelling techniques and codes developed for the simulation of flashing flows (Liao and Lucas, 2017). The techniques are often subdivided based on which assumptions are made. The assumption can be made that the phases are in thermal equilibrium and/or that the phases are in mechanical equilibrium. In the context of volumetric expanders, the mechanical equilibrium is assumed as both phases occupy the same expansion chamber or chambers. Thermal equilibrium can sometimes also be assumed when the phases are well mixed. This implies that the temperature can be assumed constant throughout the phases of the fluid mixture. In the case of assumed mechanical and thermal equilibrium the HEM is the only mentioned technique by Liao and Lucas (2017). However, as visible in the experiments of Kanno and Shikazono (2015), this is not the case in the reciprocating expander. The measured liquid temperature in these experiments is higher than the measured vapour temperature. The models that assume mechanical equilibrium, but not thermal equilibrium, are the mixture model, the boiling delay model and the HRM. These will be elaborated on further.

2.1 Mixture model

This model solves multiple continuity equations, both for the phases and/or for the mixture. In most applications 4 continuity equations are applied. Sometimes an additional equation to determine the

vapour generation rate is also required. One common equation for this is the Interfacial Exchange Model (IEM) shown in equation (1):

$$\Gamma_g = A_i \cdot \frac{\dot{q}}{L} \tag{1}$$

, where Γ_g is the vapour generation rate, $\dot{q}$ is the total heat flux to the phase interphase, L is the latent heat of evaporation and A_i is the area of the phase interphase. For reciprocating expanders this is either taken equal to the cross-sectional area of the piston or equal to the cross-sectional piston area multiplied with an agitation factor, depending on the boiling intensity and interphase deformation due to boiling. This methodology was followed by Kanno and Shikazono (2017).

2.2 Boiling delay model

The boiling delay model states that the boiling happens only with a certain degree of superheat in the liquid, when the nucleation of bubbles starts to take place. This bubble nucleation and growth also limits the eventual vapour generation rate. Two-phase mixture conservation equations are also applied, including property calculations for the metastable liquid thermodynamic properties. This modelling technique could be used in the future for detailed reciprocating expander models if accurate analytical expressions for bubble nucleation and growth in these conditions are available.

2.3 Homogeneous relaxation model

The homogeneous relaxation model (HRM) is based on the homogeneous equilibrium model (HEM) with an evaporation correction equation. The added evaporation equation introduces an empirical thermal relaxation time Θ. This is the time the unstable mixture takes to relax to equilibrium through evaporation. The HEM itself consists of the mass, momentum and energy conservation equations together with the assumption that the mixture is in equilibrium. Which thus means that the liquid temperature has the saturation temperature of the imposed pressure. The simplicity of this model means that it can be easily implemented. Yet the equilibrium assumption cannot be applied in a fast changing process such as in an expander. Therefore, the HRM can be used instead, wherein the equilibrium assumption is substituted by a vapour generation equation shown in equations (2) and (3) (Downar-Zapolski *et al.*, 1996).

$$\frac{\Gamma_g}{\rho} = -\frac{x - \bar{x}}{\Theta} \tag{2}$$

$$\Theta = \Theta_0 \cdot \epsilon^a \cdot \psi^b \tag{3}$$

, where Γ_g is the vapour generation rate, ρ the mixture density, x the actual vapour quality, $\bar{x}$ the equilibrium vapour quality, Θ the relaxation time, ϵ the void fraction and ψ the non-dimensional pressure difference. According to Downar-Zapolski *et al.* (1996) the definition of ψ depends on the pressure. For pressures under 10 bar equation (4) is used and for pressures over 10 bar equation (5) is used instead.

$$\psi = \frac{p_s - p}{p_s} \tag{4}$$

$$\psi = \frac{p_s - p}{p_c - p} \tag{5}$$

Where p_s is the saturation pressure corresponding to the liquid superheat, p is the actual pressure and p_c is the critical pressure. The values of Θ_0, a and b in equation (3) are constants that have to be fitted to experiments. The values found by Downar-Zapolski *et al.* (1996) are respectively $6.51 * 10^{-4} s$, -0.257 and -2.24 when equation (4) is used and $3.84 * 10^{-7} s$, -0.54 and -1.76 when equation (5) is used. These were found by applying the HRM to the Moby Dick experiments where flashing occurred. These experiments were chosen by the authors as they have served as the basis for understanding critical two-phase flow. The Moby Dick experiments consisted of flow in straight divergent nozzles. The HRM is

the simplest of the three models, only describing one possible way of mass exchange between the phases, yet it is still a remarkably accurate methodology.

3 MODELLING OF THERMAL NON-EQUILIBRIUM EXPANSION

3.1 HEM model as the starting point

The available model is based on the previous work of Lecompte *et al.* (2017a) and Lecompte *et al.* (2017b). This model assumed that the mixture was in equilibrium at every point. The model equations taken from this work are shortly described here.

$$m_p \cdot a = \frac{\pi D_{cyl}^2}{4}\left(p_{cyl} - p_{bp}\right) - F_{fr} - F_{load} \tag{6}$$

Herein is m_p the total piston mass, which accounts for all the masses that need to be accelerated, D_{cyl} is the inner diameter of the cylinder. p_{cyl} is the pressure within the cylinder, p_{bp} is the backpressure on the piston, which is taken equal to the atmospheric pressure. F_{fr} is the friction force between the piston and the wall according to Tran and Yanada (2013). F_{load} is the external load from an electromechanical linear motor. These forces are also represented in Figure 1. The heat transfer from the walls is expressed as equation (7):

$$\dot{Q} = h_{wall} \cdot A_{wall} \cdot \left(T_{cyl} - T_{wall}\right) \tag{7}$$

, with $h_{wall}$the heat transfer coefficient according to Woschni (1967). T_{cyl} is the vapour temperature, T_{wall} the wall temperature taken as the median of inlet and outlet temperatures and A_{wall} is the surface wall area of the current working volume. This consists of a cylindrical area and 2 circular ends.

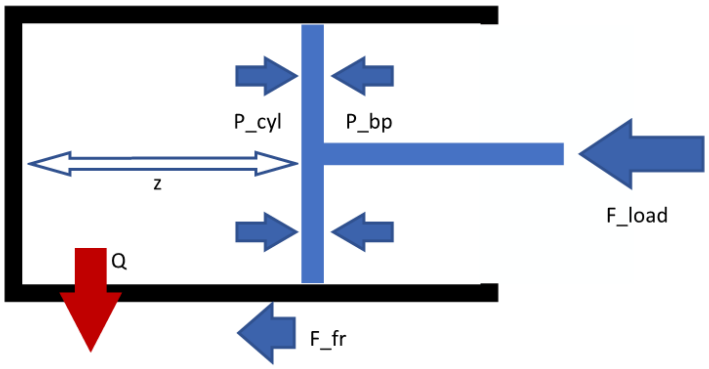

Figure 1: Simple sketch of the reciprocating expander during expansion stroke.

The inlet mass flow rate is calculated assumed as a steady-state, incompressible flow as illustrated in equation (8):

$$\dot{m} = C \cdot A_{valve} \cdot \sqrt{2 \cdot \rho_{in} \cdot \left(p_{in} - p_{cyl}\right)} \tag{8}$$

, with $\dot{m}$ the inlet mass flow rate, A_{valve} the valve throughflow area, p_{in} the pressure in the inlet tube and p_{cyl} the pressure in the piston. C is the flow coefficient taken as 0,430.

3.2 Assumptions for reciprocating expanders

The adapted model solves a system of differential equations with a given initial state. The model is run on the first half second of the intake and expansion stroke. This time is subdivided in 500 timesteps. More time steps do not alter the solution of the model while it raises the calculation time. The initial state is assumed to be the stationary piston at bottom dead center, corresponding to z equal to 2 cm in Figure 1. This initial volume is filled with saturated vapour at the exhaust saturation pressure. This follows from the assumption that the exhaust stroke removed all liquid from the working chamber, only leaving vapour in the dead volume of the expander. The initial amount of liquid mass present in the

dead volume is thus set to zero. Other design parameters of the reciprocating expander are listed in Table 1. These were assumed to be identical to the sizing of Lecompte *et al.* (2017b), which allows to easily compare simulation results.

Table 1: Values of design parameters

Parameter	Value	Dimension
Piston diameter	0.030	m
Valve orifice diameter	0.00476	m
Clearance volume	14.137	cm^3
Load profile (F_{load})	$50 \cdot V^2$	N
Piston mass	5	Kg
Closing time of valve	0.02	s
Saturation inlet temperature	150	°C
Fluid	Cyclopentane	-

As shown by Kanno and Shikazono (2015), the two-phase mixture cannot be assumed to be in equilibrium throughout the entirety of the expansion process. Therefore the available model, where instantaneous evaporation was assumed, is adapted with the use of the HRM. This modelling technique was chosen because it successfully describes complex flash boiling phenomena in a simple way, while remaining accurate (Banaszkiewicz and Kardas, 1997) to static flashing experiments. The non-equilibrium state requires the model to keep track of the state of each phase separately instead of the state of the mixture. In accordance with Kanno and Shikazono (2015) it is assumed that the heat loss, equation (7), is primarily due to the liquid phase and that the required work to move the piston is delivered by the vapour phase. The pressure within the working chamber is calculated through the assumption that the vapour phase is in equilibrium, which is a common assumption within all flash boiling models. To calculate the vapour density one more assumption was required, being that the volume change of the liquid is very small compared to that of the vapour phase as stated by Kanno and Shikazono (2015).

3.3 Implementation of HRM

In each time step the piston position and speed are known through the solver as they are a part of the system of differential equations. The change in velocity is found through the acceleration (equation (6)) while the change in piston position is the velocity by definition. The pressure at each time step is calculated through the use of Coolprop (Ian H. Bell *et al.* 2014) based on the density, calculated through the assumption of (Kanno and Shikazono, 2015), and the internal energy of the saturated vapour. The vapour temperature follows from the pressure through the saturated vapour assumption. The liquid superheat is then calculated through equations (9) and (10):

$$u_l = u_{l,sat}(p) + c_v(p) \cdot T_{sup} \tag{9}$$

$$T_l = T_g + T_{sup} \tag{10}$$

, with u_l the internal energy of the liquid in the current time step, $u_{l,sat}(p)$ is the internal energy of saturated liquid at the pressure in the time step, $c_v(p)$ is the mass specific heat at constant volume and T_{sup} is the liquid superheat. The liquid temperature follows from adding this superheat to the vapour temperature T_g as shown in equation (10). With this liquid temperature the model is able to calculate the saturation pressure corresponding to the liquid superheat, p_s, through Coolprop (Ian H. Bell *et al.* 2014). Equations (4) and (5) are used to calculate ψ based on the 10 bar pressure threshold. ϵ is calculated through equation (11) (Liao and Lucas 2017):

$$\epsilon = \frac{\rho_l - \rho}{\rho_l - \rho_g} \tag{11}$$

, in which ρ is the density of the mixture, ρ_l and ρ_g are the liquid and vapour phase densities respectively. The relaxation time, Θ, is calculated through equation (3). Due to the lack of experimental data in the area of two-phase volumetric expanders there is, at the moment of writing, no manner to fit the parameters in equation (3) for its purpose here. At this moment, the constants Θ_0, a and b in equation (3) are therefore only temporary taken as the values mentioned in section 2.3. However, they will be adapted later when the representative experiments become available. The two main reasons why the given numeric values are inaccurate in this case are as follows. Firstly, the working fluid in the Moby Dick experiments was water and there are no validations of these numeric values if other fluids are used. Secondly, the type of process is completely different. The Moby Dick experiments consisted of flow in straight divergent nozzles while this model simulates the intake and expansion stroke of a reciprocating expander. The final two variables needed for equation (2) are the actual vapour quality, x, and the equilibrium vapour quality $\bar{x}$. The actual vapour quality is calculated through equation (12) and the equilibrium vapour quality is calculated through the CoolProp (Ian H. Bell *et al.* 2014) wrapper for the current working chamber conditions.

$$x = \frac{m_g}{m_g + m_l} \tag{12}$$

m_g and m_l are the current vapour and liquid mass within the expander respectively. The vapour generation rate through evaporation, Γ_g, can now be calculated through equation (2). The change in liquid mass is the evaporated mass subtracted from the liquid mass intake, which is equal to equation (8) multiplied with one minus the inlet vapour quality. The change in vapour mass is similarly the evaporated mass added to the vapour mass intake. If the state that is calculated occurs at a time greater then the closing of the intake valve, corresponding with 0.02 seconds, than the intake mass is set equal to zero. The change of internal energy of the liquid phase is found by removing the heat losses, defined in equation (7), and the energy of the evaporated mass from the liquid intake internal energy. The change in vapour internal energy is the work done in that time step subtracted from the vapour intake internal energy and the energy of the evaporated mass in that time step. Similarly as with the inlet mass flow rate, when the calculated rate of change occurs at a time greater then the closing of the intake valve, the intake values are set to zero. The numerical solver can then solve the iterative loop through the timesteps, which is shown in Figure 2. The LSODA solver was applied here.

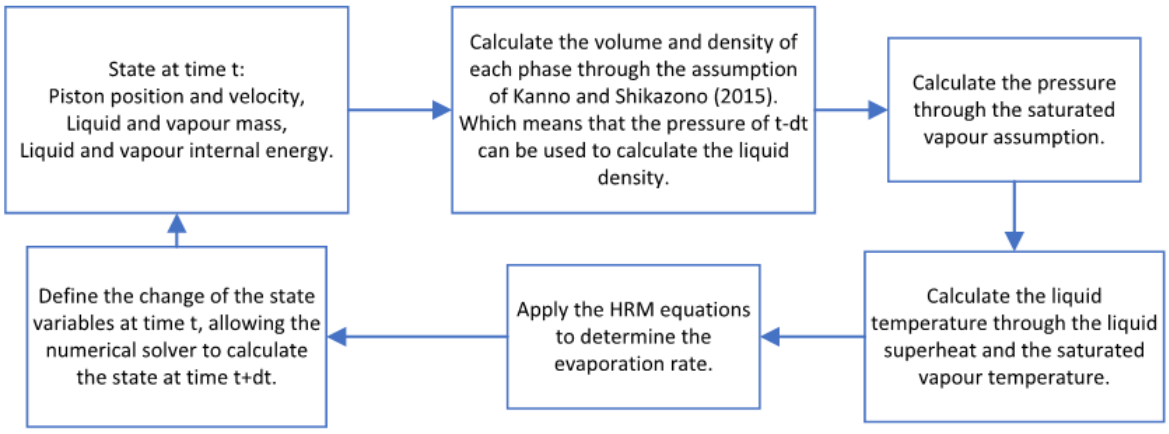

Figure 2: Simulation flowchart

4 RESULTS AND DISCUSSION

For accurate comparisons, the same expander design and inlet conditions were chosen as in the work of Lecompte *et al.* (2017a). This corresponds with an inflow of saturated liquid at a saturation temperature

of 150 °C and the parameters listed in Table 1. The working fluid was cyclopentane, of which the general data is given in Table 2.

Table 2: Thermodynamic properties of cyclopentane

Fluid	Molecular mass (g/mol)	Critical temperature (K)	Critical pressure (bar)	GWP	ODP
Cyclopentane	70.133	511.69	45.15	11	0

Some results of the model are represented in Figure 3 as the full lines. They are compared to the previous model results of Lecompte *et al.* (2017a), shown in the dashed lines. Figure 3 only shows the results of one working fluid (cyclopentane) but the same results and discussions follow from other fluids. Firstly, the load, speed and acceleration limits of the design with instantaneous evaporation are not exceeded after the implementation of the HRM. Figure 3 contains 4 subfigures. Subfigures c and d represent the pressure and displacement evolution during the intake and expansion stroke when the initial condition is equal to the exhaust condition. Herein it is visible that the working chamber pressure does not reach the pressure threshold for equation (4) given by Downar-Zapolski *et al.* (1996). Subfigures a and b are also generated and shown as comparisons to Lecompte *et al.* (2017a) and Lecompte *et al.* (2017b). These subfigures represent the same properties as in subfigures c and d, but the initial state was changed. The dead volume still only contains vapour, but the pressure is equal to the inlet pressure. The differences between both models will be discussed next.

The first difference is in the first half of the expansion process. The pressure of the model that includes the HRM is lower than the instantaneous evaporation model. This is in line with theoretical literature. The time scale is too short for the fluid to evaporate to equilibrium, resulting in less vapour within the working chamber compared to the instantaneous evaporation model. Once the inlet valve closes, at 0.02 seconds, the pressure line of the HRM simulation begins to converge to the instantaneous evaporation model simulation. The mixture of the instantaneous evaporation model is permanently in equilibrium, while the mixture of the HRM tends to equilibrium over time. Therefore, the pressure lines converge as both models will tend to the same equilibrium when infinite time is given. A result of the lower pressures during the intake stroke can be deduced from equation (8). Due to the bigger pressure difference between the working chamber pressure and the inlet pressure, there is a larger inlet mass flow rate. The higher flow rates, already larger in a TLC in comparison to an ORC, were thus underpredicted with the instantaneous evaporation model. When the mixture reaches equilibrium near the end of the simulations, the pressure is higher when using the HRM in comparison to the instantaneous evaporation model. This is a result from the previous mentioned higher flow rates. If both mixtures are in equilibrium, as is the case at the end of both simulations, and the volume is the same, than the pressure will be higher when more fluid is present within the working chamber. The same phenomena are present in subfigures b and d where the piston position is represented in function of the elapsed time since the start of the intake stroke. The stroke length at the end of the simulation is slightly higher. This is currently still within design limitations of the linear motor, but this can become problematic. Lastly the predicted power generation of the model using the HRM is 197 W compared to 214 W with the instantaneous evaporation model.
The current numerical results do rely slightly on the used definition of . Currently it is uncertain if the threshold of 10 bar found by Downar-Zapolski *et al.* (1996) also holds true for other fluids outside of water. It is possible that cyclopentane has another threshold pressure. However, changing this threshold pressure does not change the conclusions drawn here, while it does change the scale of the conclusions drawn here. Secondly the numerical values of the constants , a and b in equations (3) and (4) of the HRM also have an impact similarly to the pressure threshold. With the current numerical values and the current pressure threshold it seems like that the simulation still slightly overestimates the rate of evaporation when comparing the model with some experimental data of Kanno and Shikazono (2015). This implies that the conclusions drawn previously will be even more pronounced when the parameters are fitted to planned experiments.

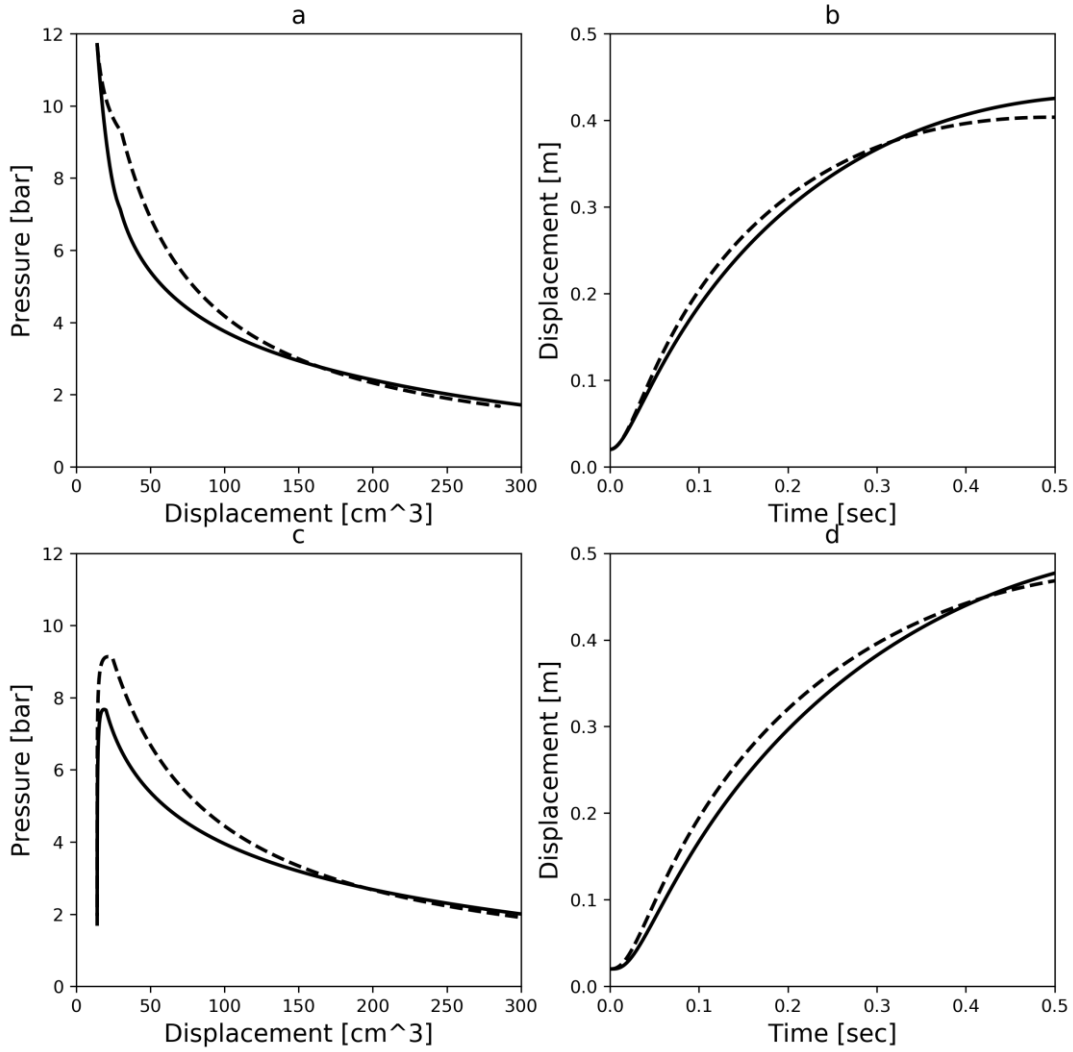

Figure 3: a) p-V diagram with initial inlet condition, b) piston displacement as a function of time with initial inlet condition, c) p-V diagram with initial outlet condition, d) piston displacement with initial outlet condition, working fluid is cyclopentane, dashed line is the instantaneous evaporation, full line is with HRM.

5 CONCLUSIONS

A previous existing instantaneous evaporation model was adapted to include the homogeneous relaxation model (HRM). Incorporating the non-equilibrium state of the fluid in the fast altering process of expansion, as the evaporation of the liquid phase is time sensitive as well. This was done with the goal to design a reciprocating expander to study the flashing phenomena in volumetric expanders for the use in trilateral cycles. The adaptations show that initial predictions with instantaneous evaporation are slightly inaccurate. The updates predict lower work and higher mass flow rates, important in the design of an experimental cycle. The restraints for the electromechanical motor do remain within design. This with rough estimations for the numeric values of the HRM parameters, due to the limited experimental data available for this type of process. The test bench design for the further planned experimental campaign will thus have to be adapted with current findings.

In future work, the methodology and implementation will be compared to the fundamentally different experiments of Kanno and Shikazono. The designed reciprocating expander will be build and the HRM variables fitted to experimental data that correlates with the current application.

REFERENCES

Banaszkiewicz, M., Kardas, D., 1997, Numerical calculations of the moby dick experiment by means of unsteady relaxation model, *J. theoretical and applied mechanics,* vol. 35, no. 2: p. 211-232.

Bell I. H., Wronski, J., Quoilin, S., Lemort, V., 2014, Pure and Pseudo-pure Fluid Thermophysical Property Evaluation and the Open-Source Thermophysical Property Library CoolProp, *Ind. Eng. Chem. Res.*, vol. 53, no. 6: p. 2498-2508.

Dipippo, R., 2007, Ideal thermal efficiency for geothermal binary plants, *Geothermics*, vol. 36, no. 3: p. 276-285.

Downar-Zapolski, P., Bilicki, Z., Bolle, L., Franco, J., 1996, The non-equilibrium relaxation model for one-dimensional flashing liquid flow, *Int. J. Multiph. Flow*, vol. 22, no. 3: p. 473-483.

Dumont, O., Dickes, R., Lemort, V., 2017, Experimental investigation of four volumetric expanders, *Energy Procedia*, vol. 129, p. 859-866.

Fischer, J., 2011, Comparison of trilateral cycles and organic rankine cycles, *Energy*, vol. 36, no. 10: p. 6208-6219.

Glavatskaya, Y., Podevin, P., Lemort, V., Shonda, O., Descombes, G., 2012, Reciprocating Expander for an Exhaust Heat Recovery Rankine Cycle for a Passenger Car Application, *Energies*, vol. 5, no. 6: p. 1751-1765.

Kanno, H., Shikazono, N., 2015, Experimental and modeling study on adiabatic two-phase expansion in a cylinder, *Int. J. Heat Mass Transf.*, vol. 86, p. 755-763.

Kanno, H., Shikazono, N., 2017, Modeling study on two-phase adiabatic expansion in a reciprocating expander, *Int. J. Heat Mass Transf.*, vol. 104, p. 142-148.

Lecompte, S., Huisseune, H., van den Broek, M., Vanslambrouck, B., De Paepe, M., 2015, Review of organic rankine cycle (ORC) architectures for waste heat recovery, *Renew. Sust. Energ. Rev.*, vol. 47, p. 448-461.

Lecompte, S., van den Broek, M., De Paepe, M., 2017(a), Design of an optical-access expansion chamber for two-phase expansion, Proceedings of *ECOS 2017- The 30th environmental conference of efficiency, cost, optimization, simulation and environmental impact on energy systems.*

Lecompte, S., van den Broek, M., De Paepe, M., 2017(b), Initial design of an optical-access piston expander chamber for wet expansion, *Energy Procedia,* vol. 129, p. 307-314.

Li, Z., Lu, Y., Huang, Y., Qian, G., Chen, F., Yu, X., Roskilly, A., 2017, Comparison study of trilateral rankine cycle, organic flash cycle and basic organic rankine cycle for low grade heat recovery, *Energy Procedia*, vol. 142, p. 1441-1447.

Liao, Y., Lucas, D., 2017, Computational modelling of flash boiling flows: A literature survey, *Int. J. Heat Mass Transf.*, vol. 111, p. 246-265.

Öhman, H., Lundqvist, P., 2013, Experimental investigation of a lysholm turbine operating with superheated, saturated and 2-phase inlet conitions, *Appl. Therm. Eng.*, vol. 50, no.1: p.1211-1218.

Tran, X., Yanada, H., 2013, Dynamic friction behaviors of pneumatic cylinders, *Intelligent Control and Autom.*, vol. 4, no.2: p.180-190.

Woschni, G., 1967, A universally applicable equation for the instantaneous heat transfer coefficient in the internal combustion engine, *SAE technical papers*, p. 3065-3083.

ACKNOWLEDGEMENT

I would like to thank the Research Foundation-Flanders for their financial support through FWO-Flanders grants (1SD9721N).

.